E7-94-147

Yu.A.Lazarev, Yu.Ts.Oganessian, Z.Szeglowski,
V.K.Utyonkov, Yu.P.Kharitonov, O.Constantinescu,
Dinh Thi Liên, I.V. Shirokovsky, S.P.Tretyakova
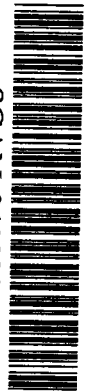
CROSS SECTIONS OF THE $(HI, \alpha n)$ CHANNEL IN THE COLD-FUSION-TYPE REACTIONS ^{209}Bi + ^{40}Ar AND ^{208}Pb + ^{37}Cl

$SW\ 9443$

SCAN-9410208

CERN LIBRARIES, GENEVA

1994

1. Introduction

It is a widely accepted fact that heavy-ion induced complete fusion reactions followed by evaporation of several neutrons from the composite system, i.e., (HI,xn) processes, were the most prolific means for producing progressively heavier nuclei in the region of transfermium elements, Z>100 (see, e.g., refs. [1–5]). Most of the transfermium nuclei known to exist to date were produced by the (HI,xn) reactions using as targets both spherical nuclei near ^{208}Pb and deformed actinide nuclei. In this way the chart of the nuclides was extended by now up to the borderline Z=109. At the same time, a drastic decrease in production cross sections is observed with increasing Z, from several microbarns at Z=102 down to some ten picobarns at Z=109. In fusion reactions between actinide targets and beams such as ^{12}C, ^{18}O or ^{22}Ne, which were used in the sixties and seventies to discover elements 102 through 106, the decreases in production cross sections are thought to be due to the severe depletion from prompt fission of the composite systems formed at excitation energies of 40 to 50 MeV already at the Coulomb barrier [1,2,3]. When making the heaviest nuclides by fusing projectiles ranging from ^{48}Ca to ^{58}Fe with targets of ^{208}Pb or ^{209}Bi nuclei, the rapid decrease in cross sections with Z is believed to be associated with a progressively stronger hindrance to fusion, where the repulsive Coulomb forces more and more dominate the fusion dynamics [2,4,5]. Whatever the nature of limitations, the cross sections for producing nuclides with Z=110 are expected to be certainly below 10 pb for any kind of (HI,xn) reactions.

In view of the above limitations known for the (HI,xn) reactions for a long time, many attempts were made in the past on exploring alternative possibilities of synthesizing the heaviest nuclei. These attempts involved a variety of heavy-ion reactions collectively referred to as "transfer reactions" of which prominent examples are

deep inelastic collisions of the $^{238}U+^{238}U$ and $^{238}U+^{248}Cm$ type [6] or ^{18}O- and ^{22}Ne-induced multinucleon transfer reactions using ^{254}Es as a target [7]. The latter turned out to be quite prolific and have resulted in the recent discovery of a number of new neutron-rich nuclides such as ^{260}Md, $^{262}102$, $^{261}103$, and $^{262}103$ [7]. An interesting suggestion for the production of new elements was formulated recently in ref. [8] by considering cold quasi-elastic multi-proton transfer reactions induced by proton-rich projectiles near to closed nucleon shells (for example ^{144}Sm) on very heavy targets (like ^{248}Cm).

Also, there were attempts to consider the productivity of heavy-ion synthesis reactions accompanied by the "direct" emission of light charged particles, particularly, (HI,αxn) reactions, in which the light particle was supposed to carry off a major portion of the intrinsic energy available for the reaction intermediate. In this way, one could hope to produce relatively colder intermediate systems showing up increased probabilities of survival against prompt fission. In particular, the potentialities of the αxn reactions[1] were discussed at some length a decade ago in ref. [1]. Some fragmentary measurements were also attempted at that time [9–13]. However, no indications in favour of the αxn reactions were found. Later on, a significant set of data was reported [14] regarding the cross sections of the pxn and αxn channels with $x\leq2$ in the reactions of ^{48}Ti, ^{49}Ti and ^{50}Ti projectiles with ^{208}Pb target nuclei. For these Ti-induced reactions, the upper cross section limits have been determined to be at the level of one hundredth of the xn cross sections in the bombarding energy range from the reaction thresholds to a maximum value of 5.5 Mev/u [14]. It seemed that these data hold out little hope of any advantages of the αxn reactions in producing the heaviest nuclei, at least for the reaction systems of the so-called cold fusion type.

Recently, however, the αxn reaction as a "possible new approach to superheavy elements" was put forward again by Nomura *et al.* [15,16]. It was stated [15] that the αxn reactions, in which a precompound α-particle emission takes place, occur significantly even near the Coulomb barrier. This statement was supported by

---

[1]To designate heavy-ion reaction channels, here and below we use shortened notations, i.e., xn or αxn instead of (HI,xn) or (HI,αxn), etc.

2

cross section measurements made for the αn and α2n channels of the ^{209}Bi+^{40}Ar reaction. These measurements were performed at an ^{40}Ar bombarding energy of 5.21 MeV/u by using the gas-filled recoil separator GARIS [17]. The observation of the α-particle-decay lines of ^{244}Cf and ^{243}Es formed via the (^{40}Ar,αn) and (^{40}Ar,α2n) channels was reported and on this basis it was stressed that the αxn reactions occur with a significant probability even in the cold-fusion type combination of target and projectile if these are allowed energetically. The cross sections for the ^{209}Bi(^{40}Ar,αn) and ^{209}Bi(^{40}Ar,α2n) reactions were determined to be surprisingly large, 44±15 nb and 36±15 nb, respectively [16]. By involving these results into a series of oversimplified considerations, Nomura *et al.* have arrived at the conclusion [15,16] that the productivity of the α2n reactions in the region of the heaviest elements can be orders of magnitude higher as compared to that known for xn reactions. For instance, a possible cross section for the ^{209}Bi(^{65}Cu,α2n)^{268}110 reaction was estimated to be as high as 1 nb [15], in a dramatic contrast with picobarn values expected [2,4,5,14] for xn reactions leading to Z=110 nuclides.

Thus, both the data and the conclusions of refs. [15,16] turned out to be in strong contradictions with what was measured or accepted as being true before.

In the present paper we report on experiments designed to clarify these contradictions by studying cross sections of the αn channel in the cold-fusion-type reactions ^{209}Bi+^{40}Ar and ^{208}Pb+^{37}Cl.

2. Experimental procedure

2.1. EXPERIMENTAL METHOD

To perform the measurements with the highest possible sensitivity and reliability, in the present experiments, in contrast to the work by Nomura *et al.* [15,16], we used the off-line radiochemistry technique instead of employing, e.g., the Dubna gas-filled recoil separator [18]. The recoil separators like those operated at RIKEN [17] or JINR [18] possess a certain (generally small) angular acceptance and are powerful

3

means for studying products from complete fusion reactions followed by neutron evaporation, which are featured by the well known, clearly defined and strongly forward-peaked kinematics. This is not the case for fusion-evaporation processes accompanied by a "direct" or "precompound" emission of particles. Kinematic features of such processes are not so well known and can be predicted only with a limited degree of confidence. At the same time, the heavy residues produced in these processes are anticipated to show significantly broader, side-peaked angular distributions and thus are expected to be suppressed by the kinematic separators by an unknown factor essentially dependent on both reaction system and bombarding energy. Therefore, to avoid uncertainties associated with kinematics, we applied the catcher technique with off-line chemical separations, which allowed all the products of interest to be collected irrespective of unknown angular distributions of these.

For our off-line α-decay measurements, the nuclide indicative of the αn channel was chosen to be the long-lived isotope ^{240}Cm with $T_{1/2}$=27 d, b_α>99.5%, E_α=6290.5 keV (71.1%) and 6247.7 keV (28.9%) [19]. As is seen from fig.1, the immediate products of the αn channel in the ^{209}Bi+^{40}Ar and ^{208}Pb+^{37}Cl reactions, ^{244}Es and ^{240}Bk, are represented by ^{240}Cm with the 100% probability. Evidently, a number of other reaction channels can also contribute to the measured yield of ^{240}Cm. These are 1n, 1p, αp, 2αn and 2αp channels in the ^{209}Bi+^{40}Ar system and 1n, 1p and αp channels in the ^{208}Pb+^{37}Cl case. Thus, the measured cumulative yield of ^{240}Cm will represent an upper cross section limit for the αn channel.

For the reactions under study, the off-line technique does not allow the $\alpha x n$ channels with x=2 and 3 to be probed with an appropriately high sensitivity since there are no suitable α-emitters in the corresponding decay chains. Yet a special remark should be made regarding xn and αxn channels with x=3. These channels lead to nuclides which can undergo spontaneous or/and electron-capture (EC)-delayed fission, see fig.1. The detection of the fission events can give thus a useful additional information, and, to obtain it, we have extended our experimental technique to a possibility of fission fragment counting.
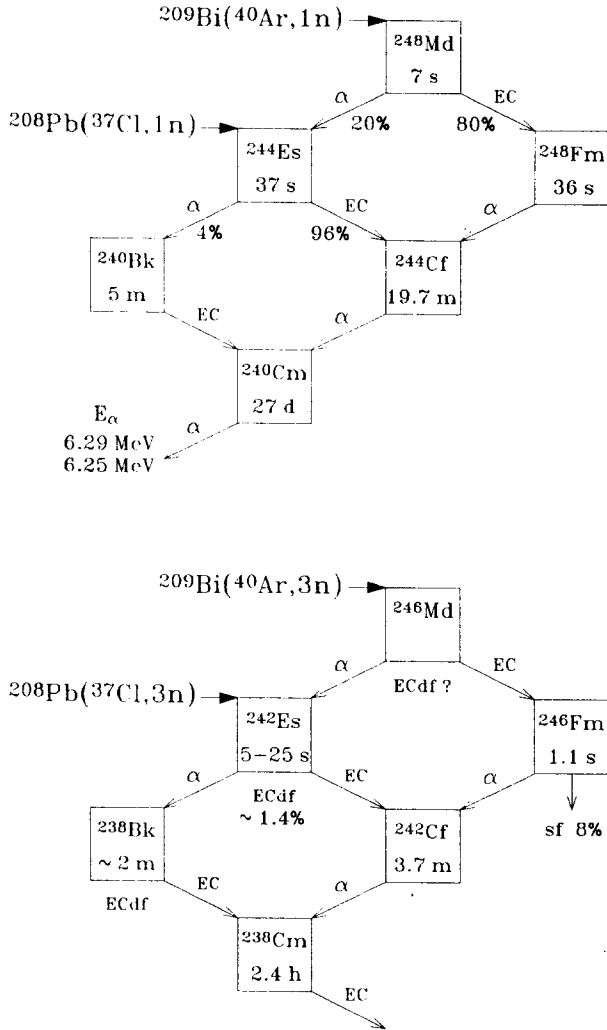
^{209}Bi(^{40}Ar,1n) →

^{248}Md

7 s

α   EC

20%   80%

^{208}Pb(^{37}Cl,1n) →

^{244}Es

37 s

^{248}Fm

36 s

α   EC   α

4%   96%

^{240}Bk

5 m

^{244}Cf

19.7 m

EC   α

^{240}Cm

27 d

E_α

6.29 MeV
6.25 MeV

α

^{209}Bi(^{40}Ar,3n) →

^{246}Md

α   EC

ECdf ?

^{208}Pb(^{37}Cl,3n) →

^{242}Es

5−25 s

^{246}Fm

1.1 s

α   EC   α

ECdf
~ 1.4%

^{238}Bk

~ 2 m

^{242}Cf

3.7 m

sf 8%

EC   α

ECdf

^{238}Cm

2.4 h

EC

Fig.1. Radioactive decay chains of the products from the ^{209}Bi+^{40}Ar and ^{208}Pb+^{37}Cl reaction channels associated with x=1 and x=3. The decay properties indicated were taken from refs. [20–22].

2.2. TARGETS AND IRRADIATIONS

The irradiations were performed at the U400 cyclotron of the JINR Laboratory of Nuclear Reactions (Dubna) by using the wheel system described in ref. [23]. A beam of ^{40}Ar or ^{37}Cl projectiles with an incident energy of 230 MeV and average intensity of about 5×10^{12} particles/s struck tangentially the lateral surface of a cooled copper cylinder onto which 2 to 3 mg/cm^2 of the metallic target material was deposited. This cylindrical target (serving simultaneously as a recoil catcher) rotated with a constant velocity. Mica fission fragment detectors arranged all around the rotating target cylinder (except for the beam input zone) were used for the detection of EC-delayed or spontaneous fission events.

The metallic layers of Bi and isotopically enriched ^{208}Pb (99.0%) were deposited onto the target cylinder by evaporation in a vacuum; a target of ^{206}Pb enriched to 94.9% was also used in one of bombardments. After end of irradiation, the entire layer of the target material was mechanically removed from the target cylinder and then was treated radiochemically to achieve element separation and prepare a thin source for α-decay measurements.

Earlier, this technique was extensively used in experiments aimed at synthesizing transfermium elements (see, e.g., refs. [14,23]) where it permitted the detection of nuclides produced with picobarn cross sections. More recently, it was employed in the experiments which led to the discovery of a new region of EC(β^+)-delayed fission around ^{180}Hg–^{188}Pb [24,25], as well as in the studies of the stability of the K-isomeric states of ^{250}Fm and ^{254}102 against spontaneous fission [26].

2.3. CHEMICAL SEPARATIONS

Three steps of chemical treatment were applied to isolate the fraction of Cf, Cm and Am from the irradiated Bi or Pb target material, the total amount of which was about 200 mg per one target wheel.

The first step was to separate lanthanide and actinide elements from the target

material. With this aim in view, the latter was dissolved in concentrated HNO_3, with adding 10 μg of La as a carrier. Also added were tracers of [160]Tb and [144]Ce as well as markers of [148]Gd, [241]Am and [244]Cm used for the chemical yield determination. The prepared solution was evaporated to a small volume and then 50 ml of 0.002M ethylene-diamine-tetraacetic acid (EDTA) buffered at pH=1.2 were added. In the case of Bi, which is known to form in acid media stable complexes with EDTA [27], a solution of 0.01M EDTA was used. The solution was heated up to 50°C and passed through a cation-exchange column filled with the resin Dowex-50, at the same temperature, to avoid crystallization of EDTA. Under these conditions, the lanthanides and actinides were absorbed on the column, whereas Bi and Pb were quantitatively eluted. After sorption, the column was washed with 100 ml of 0.002M EDTA solution buffered at pH=1.2 and then, successively, with water, with 0.2M HF, with water again, and with 2M HCl.

The second step was to purify the lanthanides and actinides absorbed on the Dowex-50 column. To this end, these were eluted with 6M HCl, evaporated to dryness, and dissolved in 0.1M HCl. The obtained solution was purified on a column with di(2-ethylhexyl) phosphoric acid (HDEHP) from which the absorbed lanthanides and actinides were eluted with 6M HCl and subsequently passed through an anion-exchange Dowex-1 column. The eluate from this column was dried and the residue, after dissolving in 0.1M HCl, was passed through a cation-exchange Aminex A-5 ($\sim$13μm) column from which the fraction of Cf, Cm and Am was eluted with α-hydroxyisobutyrate solution at pH=4. The above procedure allows decontamination factors higher than 10^8 to be obtained in purifying trivalent Am and heavier actinides from Ra, Ac, Th, U, Np, Pu, and other elements.

In the third step, thin sources were prepared for α-decay measurements. The fraction of Cf, Cm and Am from the Aminex column was finally purified using HDEHP and Dowex-1 columns and then electrodeposited onto a polished disk of stainless steel. Typically, the measured chemical yield of Cm was equal to about 85%.

2.4. ALPHA-PARTICLE SPECTROMETRY

The radiochemically prepared sources with the fraction of Cf, Cm and Am were measured in the low-background α-activity spectrometer described in ref. [28]. Along with accumulating α-particle-energy spectra, the spectrometer records also detection times of individual α-decay events. Thus, analyzing the energy-time correlations of the detected α-events makes it possible to reveal and rule out background α-events which could originate, e.g., from natural decay series involving α-emitters of the Po-Th region.

The measurements were performed in a nearly 2π counting geometry; typically, the activity spot of a 12-mm diameter was placed at a 0.7-mm distance in front of a circular 20-mm surface-barrier Si detector. The close counting geometry explains the appearance of visible low-energy tails in the profile of the recorded α-lines. For each particular case, the spectrometric detection efficiency was determined by considering the actual shape of the reference α-lines from ^{148}Gd and ^{241}Am. These reference α-lines were used also to determine the net efficiency of the chemical procedures as well as to check the stability of the spectrometer in the course of the measurements which continued (albeit with breaks) for two months or so.

3. Measurements and results

3.1. OBSERVATION OF ^{240}Cm

To study the production of ^{240}Cm, we have performed three ^{209}Bi+^{40}Ar bombardments and a bombardment of ^{208}Pb+^{37}Cl. Each of these bombardments was followed by the radiochemical treatment of the irradiated target material with subsequent α-decay measurements. A summary of experimental results is given in table 1.

Typical α-particle-energy spectra resulting from the fraction of Cf, Cm and Am are shown in fig.2 for both reactions under study. The two energy spectra are quite similar and show, with a sufficient statistics, a clear peak at $\simeq 6.3$ MeV, which should
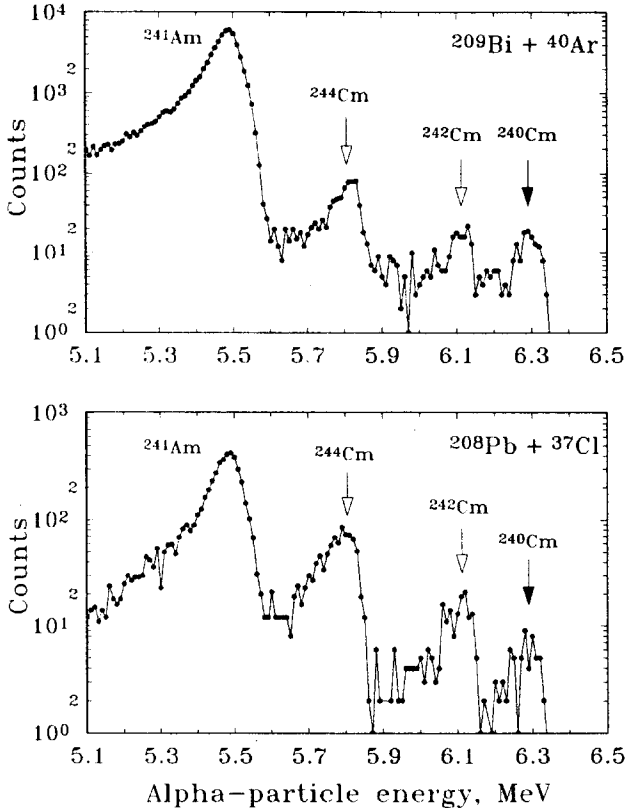
Fig.2. Alpha-particle-energy spectra from the fraction of Cf, Cm and Am isolated after ^{209}Bi+^{40}Ar and ^{208}Pb+^{37}Cl irradiations. The α-peak at $\simeq$5.5 MeV is due to the marking activity of ^{241}Am, E_α=5486 keV (85.1%) and 5443 keV (13.3%) [19], whereas the 3183-keV α-line of the ^{148}Gd marker is not included in the figure. The α-peaks at $\simeq$5.8 MeV and $\simeq$6.1 MeV are due to the marking activity of ^{244}Cm, E_α=5805 keV (76.4%) and 5762 keV (23.6%), involving an admixture of ^{242}Cm, E_α=6113 keV (74.1%) and 6069 keV (25.9%) [19].
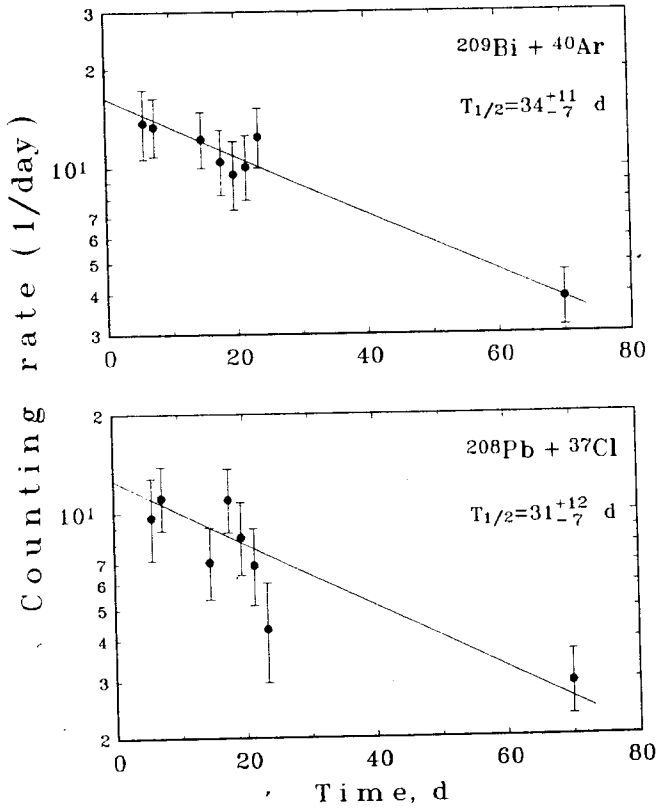
Fig.3. Decay of the $\simeq$6.3-MeV α-activity from the fraction of Cf, Cm and Am isolated after ^{209}Bi+^{40}Ar and ^{208}Pb+^{37}Cl irradiations. Statistical errors are shown by vertical bars. The indicated half-life values were determined by the maximum likelihood method [29].

be assigned to ^{240}Cm. Apart from the coincidence with the α-particle energy known for ^{240}Cm, this assignment of the peak is strongly supported by quite a number of other arguments. The argument of prime importance is provided by the fact of the preceding chemical isolation of the Cf-Cm-Am fraction. In second, the measurements

Table 1

Experimental results on the production of ^{240}Cm in the ^{209}Bi+^{40}Ar and ^{208}Pb+^{37}Cl reactions at $E_{lab} \leq 230$ MeV

Reaction	I [a)	N_α [b)	Y(^{240}Cm) [c)	$\sigma(^{240}$Cm) [d) (nb)
^{209}Bi+^{40}Ar	0.8	40	$2.3^{+1.0}_{-0.9}$	0.6 ± 0.3
	0.7	80	$1.9^{+0.8}_{-0.7}$	$0.5^{+0.3}_{-0.2}$
	2.0	176	$1.7^{+0.5}_{-0.4}$	0.5 ± 0.2
^{208}Pb+^{37}Cl	2.1	130	2.5 ± 0.8	0.6 ± 0.3

a) Beam dose in units of 10^{18} incident particles.

b) Number of α particles detected in the $\simeq$6.3-MeV α-group.

c) Thick-target yield of ^{240}Cm (i.e., yield per one beam particle) in units of 10^{-15}; the total detection efficiency is taken into account in the determination of Y.

d) Estimated assuming ΔE_{FWHM}=8$\pm$2 MeV for the corresponding excitation function.

performed over a period of some 70 d allow us to follow the decay of $\simeq$6.3-MeV α-activity and thus to estimate its half-life. The corresponding decay data are presented in fig.3 and show a reasonably good agreement with the half-life value known for ^{240}Cm. Third, no time correlations were revealed between the $\simeq$6.3-MeV α decays and subsequent α events detected within a time interval of some tens of seconds; moreover, no α events were detected in the α-energy region of $\approx$6.35 to $\approx$10 MeV. This allows us to eliminate a possible contribution from ^{220}Rn (E_α=6288 keV, $T_{1/2} \simeq$56 s [19]) appearing in the decay series of natural thorium

(note that the α decay of ^{220}Rn should be followed by the α decay of the 0.15-s isotope ^{216}Po with E_α=6778 keV [19]). Finally, with reference to table 1, we stress a good reproducibility of the results obtained from the repeated bombardments. All in all, there are good grounds to conclude that the $\simeq$6.3-MeV α-group belongs to the decay of ^{240}Cm.

The measured "thick"-target yields of the $\simeq$6.3-MeV α-activity were used to estimate the effective production cross sections of ^{240}Cm in the reactions under study. To obtain these estimates, one needs to make an assumption regarding the width(s) of the corresponding excitation function(s), ΔE_{FWHM}. With a ΔE_{FWHM} value of 8$\pm$2 MeV, the effective ^{240}Cm production cross sections were estimated to be 0.5$\pm$0.2 nb and 0.6$\pm$0.3 nb for the ^{209}Bi+^{40}Ar and ^{208}Pb+^{37}Cl reactions, respectively. Using larger ΔE_{FWHM} values will evidently lower down the above cross section values.

3.2. EC-DELAYED AND SPONTANEOUS FISSION ACTIVITIES

An interesting finding of the present experiments is the observation of relatively strong EC-delayed and spontaneous fission activities in the reactions under study. The production of fissioning nuclides in these reactions has never been studied before; moreover, this is true for the production of any evaporation residues by these reactions, with the exception of experiments [30] where the ^{209}Bi+^{40}Ar reaction was used to produce the isotope ^{247}Md. Therefore to characterize the fission effects in more detail, we carried out a number of additional bombardments without chemical separations. Specifically, we performed three ^{209}Bi+^{40}Ar bombardments at different periods of the target wheel revolution, T_{rev}=9, 48, and 110 s, as well as three ^{208}Pb+^{37}Cl bombardments, with T_{rev}=48, 110, and 770 s; there was also one bombardment ^{206}Pb+^{37}Cl performed at T_{rev}=105 s. Table 2 presents summarized results from these bombardments made at $E_{lab} \leq$230 MeV.

A general pattern of the fission effects observed is seen from table 2 and fig.4. With good statistics, fission events were detected in all the three reactions in a time

Table 2

Estimated half-lives $T_{1/2}$ and production cross sections σ_{df} of the delayed fission activities observed in the reactions under study

Reaction	I [a)	N_{df} [b)	$T_{1/2}$ [c)	σ_{df} [d) (nb)
$^{209}\text{Bi}+^{40}\text{Ar}$	4.0	1301	$0.8^{+1.5}_{-0.7}$ s	$0.04^{+3.0}_{-0.02}$
			7^{+3}_{-2} s	0.14 ± 0.04
			~2 m	0.03 ± 0.02
$^{208}\text{Pb}+^{37}\text{Cl}$	2.7	1588	8^{+13}_{-3} s	0.19 ± 0.06
			$2.0^{+1.5}_{-0.5}$ m	0.08 ± 0.03
$^{206}\text{Pb}+^{37}\text{Cl}$	0.9	561		0.2

a) Beam dose in units of 10^{18} incident particles.

b) Total number of detected fission events.

c) Deduced by using the maximum likelihood method [29]; the indicated errors of $T_{1/2}$ reflect statistical uncertainties only.

d) Estimated assuming $\Delta E_{FWHM}=10\pm2$ MeV for the corresponding excitation function.

range extending from about 1 s to some 10 m. Evidently, several activities should contribute to form the observed pattern of fission events. Under given experimental conditions, the fission events appearing in the reactions we study should be associated predominantly with the x=3 channel which is expected to have the largest cross
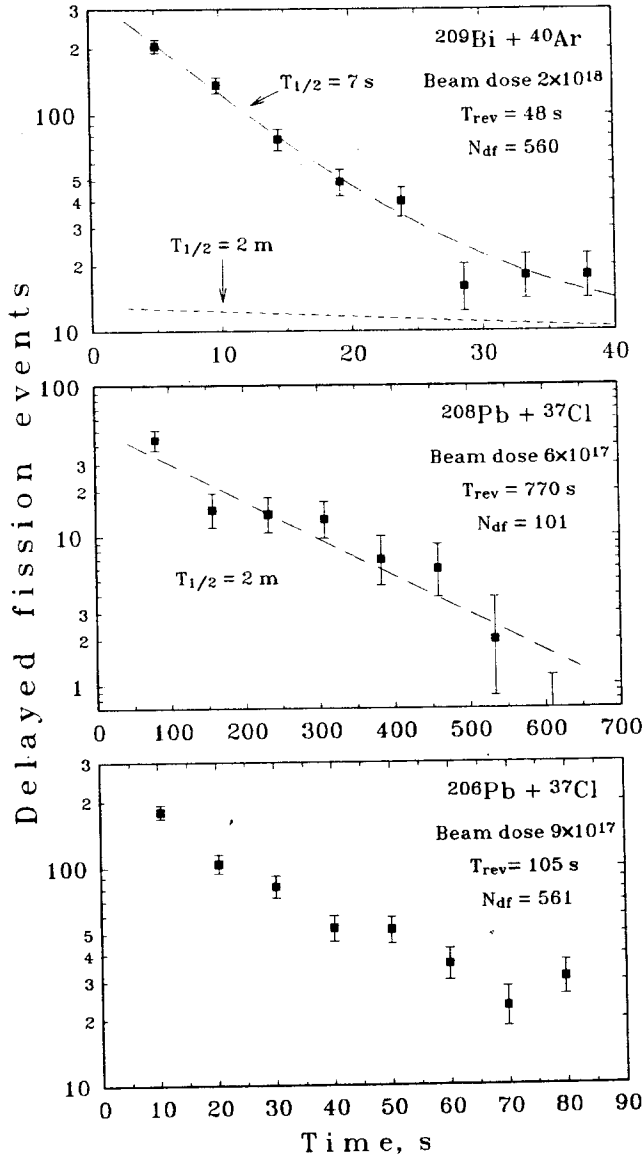
Fig.4. Time distributions of delayed fission events detected in some particular bombardments $^{209}Bi+^{40}Ar$, $^{208}Pb+^{37}Cl$ and $^{206}Pb+^{37}Cl$. See also table 2.

14

section, as can be inferred from careful studies of the very similar reaction systems ^{206,207,208}Pb+^{40}Ar [30–34]. Besides, several particular products of the x=3 channel are known or can be expected to have fission branches at the percent level (see fig.1), which is not the case for the channels of x=1, 2, and 4. However, in view of the extremely high sensitivity of the present experiments, some contributions from the x=5 channel products of the ^{209}Bi+^{40}Ar and ^{208}Pb+^{37}Cl reactions should not be ruled out completely. This is hinted also by the observations from the ^{206}Pb+^{37}Cl bombardment. All in all, there is quite a number of potential sources of the fission events detected. This makes the problem of disentangling the fission activities to be rather complicated.

When considering the fission data more specifically, we should point out at first a fission activity with a half-life of about 7 s appearing in the ^{209}Bi+^{40}Ar and ^{208}Pb+^{37}Cl reactions (see fig.4). The most probable explanation of this activity seems to be the EC-delayed fission in the decay chain ^{242}Es$\xrightarrow[\approx 7\ s]{EC}$^{242}Cf. This explanation is in line with an observation [21] made at Darmstadt with SHIP in the ^{205}Tl+^{40}Ar reaction, where on the basis of three detected fission events the EC-delayed fission in the ^{242}Es$\xrightarrow{EC}$^{242}Cf chain was reported and its probability P_{df} evaluated to be $(1.4\pm0.8)\times10^{-2}$. The production cross section of the new isotope ^{242}Es with $T_{1/2}=5$ to 25 s was reported to be 40 nb, whereas that for the EC-delayed fission events was estimated to be 180 pb [21].

Again, a fission activity with $T_{1/2}= 2.0^{+1.5}_{-0.5}$ m can be singled out from our data. It is clearly seen in the results from the ^{208}Pb+^{37}Cl bombardment made at $T_{rev}=770$ s (see fig.4). This is a new fission activity since it, despite the similar half-life, cannot be explained by EC-delayed fission in the decay chain ^{240}Bk$\xrightarrow[\sim 4\ m]{EC}$^{240}Cm, which is known to occur with a very small probability, $P_{df} \simeq 10^{-5}$ [35] or $(1.3^{+0.8}_{-0.7})\times10^{-5}$ [36]. Note that according to our measurements described in section 3.1, the ^{240}Bk production cross section in the ^{208}Pb+^{37}Cl reaction does not exceed 0.6 nb. In addition, the new fission activity cannot be due to spontaneous fission of the 3.68-m isotope ^{242}Cf since our direct experiments [37] have shown the spontaneous fission branch for

^{242}Cf to be very small, $b_{sf} \lesssim 1.4 \times 10^{-4}$. With the above facts taken into account, the most probable origin of the 2-m fission activity seems to be the EC-delayed fission in the decay chain ^{238}Bk$\xrightarrow{EC}$^{238}Cm, for which higher probability P_{df} can be expected as compared to the ^{240}Bk$\xrightarrow{EC}$^{240}Cm case. With this assignment, using the data of ref. [21] on the production and decay properties of ^{242}Es (the parent of ^{238}Bk), we obtain an order-of-magnitude estimate $P_{df} \simeq 3 \times 10^{-3}$ for the ^{238}Bk$\xrightarrow[2\,m]{EC}$^{238}Cm chain. This P_{df} value will be slightly lower if there is a contribution from spontaneous fission of ^{240}Cf [37] to the 2-m activity; although this contribution seems to be improbable, it should, strictly speaking, be excluded by way of experiments. Finally, we note that the occurrence of EC-delayed fission in the ^{238}Bk$\longrightarrow$^{238}Cm chain was reported also in ref. [22] where a fission activity with $T_{1/2}=2.4\pm0.1$ m and $P_{df}=(4.8\pm2.0)\times10^{-4}$ was produced in the reaction ^{241}Am+^{4}He (75 MeV).

In the ^{209}Bi+^{40}Ar reaction, there seem to be observed also fission events with $T_{1/2}$ of about 1 s. Such an activity can appear due to the 8% spontaneous fission branch of ^{246}Fm [20], see fig.1. A contribution to the $\sim$1-s fission events can come also from EC-delayed fission in the ^{246}Md$\xrightarrow[\sim1\,s]{EC}$^{246}Fm chain. According to systematics [38], the unknown isotope ^{246}Md is expected to be an α emitter with $T_{1/2}$ of just about 1 s and some 15% branch for EC(β^+) decay. Unfortunately, obtaining more definite information about the $\sim$1-s fission events is hindered by the presence of the intense $\approx$7-s fission activity attributed to EC-delayed fission in the ^{242}Es$\xrightarrow[\approx7\,s]{EC}$^{242}Cf chain.

A considerable fission yield was revealed also in the ^{206}Pb+^{37}Cl reaction. It is probable that two or even more fission activities contribute to the decay curve observed in this case (see fig.4). More bombardments are required to characterize these activities and make definite assignments. In principle, the ^{206}Pb+^{37}Cl reaction appears to be a probe for EC-delayed and spontaneous fission effects in the decay chains ^{240}Es$\xrightarrow{EC}$^{240}Cf and ^{236}Bk$\xrightarrow{EC}$^{236}Cm.

4. Discussion

As noted in section 2.1, our measured cross sections for the production of ^{240}Cm represent upper cross section limits for the αn channel of the ^{209}Bi+^{40}Ar and ^{208}Pb+^{37}Cl reactions. In table 3 these upper limits are compared with the αn and α2n cross section values reported by Nomura $et\ al.$ [15,16]. Also included in table 3 are αxn cross section data reported for a number of similar reaction systems of the cold-fusion type [11-14]. It is seen that our upper αn cross section limit for the ^{209}Bi+^{40}Ar reaction is two orders of magnitude lower than the value obtained in refs. [15,16].

Moreover, the main source of ^{240}Cm detected in our measurements seems to be the 1n-evaporation channel of the reactions under study, for which the so-called minimum excitation energy E^*_{min} of the composite systems (i.e., the excitation energy at the Bass fusion barrier B^{Bass}_{lab} [39]) is calculated to be about 32 MeV, like that for the well studied nearby systems ^{207,208}Pb+^{40}Ar. For cold-fusion-type reaction systems close to those examined in the present work, the only previous cross-section measurement for the 1n-deexcitation channel was attempted [31] in the ^{207}Pb+^{40}Ar reaction (E^*_{min}=31.3 MeV), with the result $\sigma^{max}_{1n} \leq 0.1$ nb[2], which is not far from our values, 0.5±0.2 nb and 0.6±0.3 nb for the ^{209}Bi+^{40}Ar and ^{208}Pb+^{37}Cl reactions with E^*_{min}=31.5 MeV and 32.4 MeV, respectively. Note that, for the cold-fusion-type reactions, even small variations in E^*_{min} values are known to lead to appreciable changes in the cross sections of particular xn-evaporation channels. Thus, taking the 1n-evaporation channel into account, our upper αn cross section limits for the reactions under study should be lowered down further compared to those given in table 3.

As to the surprisingly large cross section values reported in refs. [15,16] for the αn and α2n channels of the ^{209}Bi+^{40}Ar reaction, a reason for this seems to lie in misinterpretation of the α-particle-energy spectra recorded with poor statistics by

---

[2]Please note an evident misprint in the last line of table 1 in ref. [31]. This misprint was reproduced also in tables 2 and 3 of ref. [34], yet it was corrected in ref. [40]. The correct result is just $\sigma^{max}_{1n} \leq 0.1$ nb.

Table 3

Summary of experimental data on αxn cross sections for cold-fusion-type reactions on Tl, Pb, and Bi target nuclei

Reaction	E_{lab} [a)] (MeV)	E_{lab}^{Bass} [c)] (MeV)	E^* [d)] (MeV)	$\sigma_{\alpha xn}$ (nb)	Reference
^{208}Pb(^{37}Cl,αn)^{240}Bk	230	179.4	75.4	<0.6	present study
^{209}Bi(^{40}Ar,αn)^{244}Es	230	193.1	62.5	<0.5	present study
^{209}Bi(^{40}Ar,αn)^{244}Es	208 [b)]	193.1	44.3	44±15	[16]
^{209}Bi(^{40}Ar,α2n)^{243}Es	208 [b)]	193.1	44.3	36±15	[16]
^{204}Pb(^{48}Ca,α2n)^{246}Fm	235	216.5	38.0	<2	[12,13]
^{205}Tl(^{45}Sc,α2n)^{244}Fm	240	224.2	50.9	≤0.1	[11,12]
^{203}Tl(^{45}Sc,α)^{244}Fm	240	225.1	49.6	≤0.2	[11,12]
^{208}Pb(^{50}Ti,α2n)^{252}102	273	238.2	50.2	<0.06	[14]
^{208}Pb(^{49}Ti,αn)^{252}102	271	238.1	53.1	≤0.004	[14]
^{208}Pb(^{48}Ti,α)^{252}102	259	237.9	46.1	≤0.003	[14]

a) Laboratory energy of beam particles entering an "infinitely thick" target characteristic of experimental techniques used in refs. [11–14] as well as in the present study.

b) Bombarding energy used in ref. [16].

c) Bass fusion barrier calculated according to ref. [39].

d) Compound-nucleus excitation energy corresponding to the indicated E_{lab} value.

18

using the gas-filled recoil separator GARIS. In these measurements, the α decay of the primary αn product, the 37-s isotope ^{244}Es with $b_{EC}=0.96^{+0.02}_{-0.03}$ [41], could not be observed because of the very small α-decay branch. The identification of the αn channel was made on the basis of some six α-counts with energies of 7.16 and 7.21 MeV, taken, with a delay of 0.8 s, during the beam-off periods; note that pulsed ^{40}Ar beams were used in the experiments [15,16], with time structures of 40-s (or 10-s) beam-on/40-s (or 10-s) beam-off periods. The above counts were tentatively assigned to the α decay of the 19.7-m daughter nucleus ^{244}Cf. This assignment was based on the measured α-particle energies only, without any time information. Besides, in the measured α-spectrum there is present the very strong 7.27-MeV α-line due to the 25-s transfer product ^{211m}Po, which produces a background comparable with the number of the α-counts attributed to ^{244}Cf (see fig.4 in ref. [15] and fig.6 in ref. [16]). In a similar way, the identification of the α2n channel was made on the basis of some six 7.89-MeV α-counts collected during the beam-off periods. The half-life was not measured, but it was noted that three 7.89-MeV counts fell in the region of t>5 s after the end of the beam-on period, which probably rules out a contribution from the 0.12-s transfer product ^{212m}At with $E_\alpha \simeq 7.84$ and $\simeq 7.90$ MeV. These α-counts were attributed to the 21-s isotope ^{243}Es which is known to have $E_\alpha=7.89\pm0.02$ MeV and $b_\alpha>30\%$ [41]. In turn, the production of ^{243}Es was considered to be a signature of the α2n channel. However, this identification of the α2n channel does not seem to be unambiguous again. First, at the ^{40}Ar bombarding energy of 208 MeV, the isotope ^{243}Es could be produced, with a non-negligible cross section, via the 2n-evaporation channel. Second, apart from possibilities associated with a variety of transfer products, one very probable possibility would be to attribute the 7.89-MeV α-counts to the lighter isotopes of einsteinium, ^{242}Es and ^{241}Es, which were shown to be 5- to 25-s α-emitters with $E_\alpha \simeq 7.85$ and $\simeq 7.93$ MeV [21] and could be formed via the 3n- and 4n-evaporation channels of the ^{209}Bi+^{40}Ar reaction. At the ^{40}Ar bombarding energy of 208 MeV, the 3n channel of the ^{209}Bi+^{40}Ar reaction is quite probable, as can be inferred, e.g., from the excitation functions measured for the 3n

channel of the ^{207,208}Pb+^{40}Ar reactions [32,33]. The more so, the collection efficiency of the recoil separator GARIS for the xn-evaporation residues was measured to be 2.5 times larger than that for the αxn products, 30% instead of 12% [15,16]. Summing up, we conclude that there are no good grounds to interpret the above experimental data in favour of the αn and α2n reaction channels.

In the context of the present discussion, we cannot but pay an attention to the paper by Orlova *et al.* [42] reporting on the experimental studies of the production of evaporation residues in the reactions of ^{48}Ca projectiles with targets made of ^{nat}Tl, ^{208}Pb, and ^{209}Bi. By applying an off-line radiochemical technique, thick-target yields of the long-lived, α-decaying nuclides ^{246}Cf, ^{252}Fm+^{255}Fm, and ^{254}Fm were measured and used to characterize cross sections for different evaporation channels of the above reactions; these experimental data were included also in the conference report [43]. Along with the new interesting experimental information about the xn channels in the ^{48}Ca-induced cold fusion reactions, the paper [42] offered also quite a number of speculations as well as standard statistical-model calculations made with an ALICE code. Albeit implicitly, these latter lay an emphasis on the importance of αxn and pxn de-excitation channels in the fusion-evaporation reactions induced by ^{48}Ca. However, a careful examination of the very data reported in paper [42], as well as any other data relevant to the problem, shows that there is no evidence at all which could support the guesses and calculations of ref. [42] associated with αxn and pxn channels. To demonstrate this, in table 4 we present an up-to-date summary of the available data on xn-evaporation channels of the cold fusion reactions induced by ^{48}Ca projectiles on target nuclei of ^{203,205}Tl, ^{208}Pb, and ^{209}Bi [13,26,33,42,44-47]. In particular, the data of ref. [42] are included in table 4 without any exception. It can be seen from table 4 that there is a reasonably good agreement between the results obtained in different works. Even more important is the fact of a good agreement between the off-line radiochemical measurements performed with long-lived daughter and grand-daughter products and the on-line measurements carried out with the primary reaction products. Finally, referring to table 4, we stress that

Table 4

Summary of maximum cross sections σ_{xn}^{max} measured for xn-evaporation channels of the ^{48}Ca-induced cold-fusion reactions on Tl, Pb, and Bi target nuclei

Reaction	E_{lab} [a] (MeV)	E_{lab}^{Bass} [c] (MeV)	E^* [d] (MeV)	Detected nucleus	σ_{xn}^{max} (nb)	Ref.
^{205}Tl(^{48}Ca,n)^{252}Md	223	213.2	31.4	^{252}Fm	35±13 [e,f]	[42]
^{205}Tl(^{48}Ca,3n)^{250}Md $\Big\}$	223	213.2	31.4	^{246}Cf	145±40 [g]	[42]
^{203}Tl(^{48}Ca,n)^{250}Md		214.1	31.3			
^{204}Pb(^{48}Ca,γ)^{252}102	235	216.5	38.0	^{252}102	<0.5	[13]
^{206}Pb(^{48}Ca,2n)^{252}102	235	215.6	37.9	^{252}102	500	[13]
	215 [b]		21.7	^{252}102	190±32	[44,45]
	248		48.3	^{252}102	500±200	[26]
^{207}Pb(^{48}Ca,3n)^{252}102	235	215.2	37.2	^{252}102	~100	[13]
^{208}Pb(^{48}Ca,n)^{255}102	224	214.7	28.2	^{255}Fm [h]	420±130 [e,i]	[42]
	231		34.2	^{255}Fm [h]	130±60	[26]
	210 [b]		16.7	^{255}Fm [h]	260±30	[47]
^{208}Pb(^{48}Ca,2n)^{254}102	224	214.7	28.2	^{254}Fm	4700±1000 [e,j]	[42]
	224		28.2	^{246}Cf	4900±900 [e,j]	[42]
	214 [b]		19.7	^{246}Cf	3300±370 [k]	[47]
	231		34.2	^{246}Cf	1700±700	[26]
	213 [b]		19.3	^{254}102	2340±540	[47]
	227 [b]		30.7	^{254}102	3400±400	[33]
	215 [b]		20.9	^{254}102	390±70	[44,45]

Table 4 (continued)

Reaction	E_{lab} [a)	E_{lab}^{Bass} [c)	E^* [d)	Detected nucleus	σ_{xn}^{max}	Ref.
	(MeV)	(MeV)	(MeV)		(nb)	
^{208}Pb(^{48}Ca,3n)^{253}102	231	214.7	34.2	^{253}Es	100^{+260}_{-50}	[26]
	225 [b)		28.8	^{253}Es	109±33	[47]
^{208}Pb(^{48}Ca,4n)^{252}102	235	214.7	37.2	^{252}102	~20	[13]
^{209}Bi(^{48}Ca,n)^{256}103	212 [b)	217.5	17.6	^{256}103	61±20	[47]
	236		36.8	^{252}Fm+^{255}Fm	76±30 [e,i,l)	[42]
^{209}Bi(^{48}Ca,2n)^{255}103	215 [b)		19.6	^{255}103	437±96	[47]
	236		36.8	^{252}Fm+^{255}Fm	600±360 [e,i,l)	[42]
^{209}Bi(^{48}Ca,3n)^{254}103	227 [b)		29.4	^{254}103	28±11	[47]
	236		36.8	^{246}Cf	40±12 [e,m)	[42]

a) Laboratory energy of beam particles entering an "infinitely thick" target characteristic of experimental techniques used in refs. [13,26,42].

b) Bombarding energy corresponding to the maximum of the excitation function.

c) Bass fusion barrier calculated according to ref. [39].

d) Compound-nucleus excitation energy corresponding to the indicated E_{lab} value.

e) Our estimate obtained on the basis of the experimental data of ref. [42] by assuming ΔE_{FWHM}=8±2, 9±1, and 10±2 MeV for 1n-, 2n-, and 3n-evaporation channels, respectively, according to excitation function measurements performed in refs. [32,33,44–46].

f) Obtained by taking into account the 70.5-% abundance of ^{205}Tl in the natural thallium.

Table 4 (continued)

g) Our estimate obtained on the basis of the experimental data of ref.[42] by using the value 0.994 [20] for the total probability of the decay chain leading from ^{250}Md to ^{246}Cf and by assuming $\Delta E_{FWHM}=9\pm2$ MeV for the effective excitation function. Due to the presence of two isotopes in the natural thallium used as target in ref. [42], the given cross section estimate represents in fact the quantity $(0.705\sigma_{3n}^{max}+0.295\sigma_{1n}^{max})$. If we assume that σ_{1n}^{max} for the ^{203}Tl(^{48}Ca,n)^{250}Md reaction does not exceed 35±13 nb, we obtain an estimate of $\sigma_{3n}^{max}=170^{+60}_{-40}$ nb for the reaction ^{205}Tl(^{48}Ca,3n)^{250}Md.

h) As argued in ref. [26], yields of the (^{48}Ca,γ) and (^{48}Ca,α) reactions leading to ^{252}Fm are expected to be much lower compared to that of the reaction (^{48}Ca,n); see also ref. [47].

i) Obtained by using the empirical values [20] for b_{EC} of ^{255}Md and ^{255}102, 0.93 and 0.384, respectively.

j) Obtained by using the branching ratios $b_{EC}(^{254}102)=0.1$ and $b_\alpha(^{254}102)=0.9$ [42,48].

k) Average of two measurements performed in ref.[47].

l) Obtained by using $b_{EC}(^{255}103)=0.23$ from systematics [38] as well as measured cross sections σ_{1n}^{max} and σ_{2n}^{max} from ref. [47] in estimating σ_{2n}^{max} and σ_{1n}^{max}, respectively.

m) Obtained by using the value 0.97 [20,45,48,49] for the total probability of the decay chain leading from ^{254}103 to ^{246}Cf.

all the experimental data of ref. [42] can be quite naturally explained without appealing to αxn and pxn channels. This is why the reaction systems studied in ref. [42], with the particular long-lived nuclides chosen there for the off-line measurements, cannot be used for a sensitive probing of the αxn and pxn channels. A comparison of the cross section data shown in table 4 with the upper αxn cross section limits collected in table 3 makes this point to be completely clear.

5. Conclusions

Thus, our experiments have shown positively that the cross sections of the αxn channel in the ^{209}Bi+^{40}Ar and ^{208}Pb+^{37}Cl reactions are small, well below 0.5 nb. Our results are in accord with the bulk of the presently existing experimental data on the αxn cross sections for cold-fusion-type reaction systems [11–14,50]. As table 3 shows, these existing data form in fact a collection of upper cross section limits – the αxn cross sections are so small that no αxn product was unambiguously detected until now in fusion-evaporation reactions induced by projectiles ranging from ^{37}Cl to ^{50}Ti on targets of Tl, Pb, and Bi nuclei. Even if the energy available in these reaction systems allows the emission of an α particle, the probability of the α-particle emission turns out to be very small, by at least one or two orders of magnitude smaller than that of neutron emission; this statement is true for the proton emission as well. Clearly, in such a case, there are no grounds to rely on the αxn reactions as processes offering a more productive way to superheavy elements, as it was suggested in refs. [15,16]. Let us mention that in the very massive systems, where fusion of the partners is severely hindered by the dynamical ("extra-push") reasons associated with the excessively strong Coulomb forces, the loss of an α particle during the amalgamation stage may increase the fusion probability of the remainder, as hinted by observations [51] made in the system ^{110}Pd+^{110}Pd$\rightarrow^{220}$U. However, this cannot help much since the probability of an early α-particle emission is expected to be very small (it was estimated to be of the order of 10^{-4} for the neutron-poor ^{110}Pd+^{110}Pd system [51]) and, besides, the α emission reduces Z value of the evaporation residues produced.

The extremely low cross sections of the αxn channels, with the concurrence of much more probable xn channels, cause serious difficulties in identifying the former in experiments. As shown in section 4, the data of refs. [15,16] do not represent the material necessary for an unambiguous identification of the αn and α2n channels and can readily be explained without appealing to the α-particle emission. The same is

true for the experimental data of ref. [42] on the ^{48}Ca-induced fusion-evaporation reactions. Yet, there is a need to understand better particular reasons for the very low probabilities of the αxn channels in the cold-fusion-type reactions. Therefore further, more extensive experimental and theoretical studies of the αxn channels are certainly called for.

All what has been said above on the low probabilities of αxn channels concerns the cold-fusion-type reaction systems formed of ^{37}Cl, ^{40}Ar, and heavier projectiles and near-magic Tl, Pb, and Bi target nuclei. However an opposite situation had long been known to take place for the reactions induced by lighter projectiles like ^{12}C or ^{16}O on actinide and other target nuclei. In these reactions, formation cross sections of αxn products are often much larger compared to those of xn-evaporation residues (see, e.g., refs. [52-54] and references therein). These observations seem to be reasonably explained by mechanisms involving transfers of α-particle-like clusters (C, Be, He) from projectile to target [53,54]. Note that this α-particle structure of projectiles tends to disappear when going from ^{12}C or ^{16}O to heavier bombarding species. Another well-known and quite understandable case of the enhanced α-particle and proton emission is that characteristic of very proton-rich composite systems (see, e.g., refs. [55–57]). Here, αxn and pxn products generally dominate reaction yields, regardless of projectiles used to induce these reactions. There can probably be also some other reaction types characterized by an enhanced charged-particle emission. Considering the above-mentioned reaction groups is certainly beyond the scope of the present paper. The only remark we make here is that different groups of the αxn phenomena should be treated separately because the underlying physics is expected to be rather different. Just the contrary was the case in refs. [15,16] where conclusions concerning potentialities of the αxn reactions were drawn by considering, on an equal footing, several different groups of the αxn processes mentioned above (see fig.2 in ref. [15] or fig.4 in ref. [16]).

Finally, we would like to stress that the cold-fusion-type reactions studied in the present work could definitely be used further to produce and study new neutron-

poor Md, Es, and Bk nuclides via the xn-evaporation channels of x=2, 3, 4. The observation of the new EC-delayed fission activities described in section 3.2 of the present paper is but one example of these potentialities.

References

[1] Yu.Ts. Oganessian and Yu.A. Lazarev, Pure Appl. Chem. **53** (1981) 925

[2] Yu.Ts. Oganessian and Yu.A. Lazarev, in Treatise on heavy-ion science, ed. D.A. Bromley, vol. 4 (Plenum Press, New York, 1985) pp.3–251

[3] G.T. Seaborg and W.D. Loveland, in Treatise on heavy-ion science, ed. D.A. Bromley, vol. 4 (Plenum Press, New York, 1985) pp.255–330

[4] P. Armbruster, Ann. Rev. Nucl. Part. Sci. **35** (1985) 135

[5] G. Münzenberg, Rep. Prog. Phys. **51** (1988) 57

[6] G. Herrmann, Pure Appl. Chem. **53** (1981) 949; Angew. Chem. Int. Ed. Engl. **27** (1988) 1417

[7] E.K. Hulet, Proc. Int. School-Seminar on heavy ion physics, Dubna 1989, report D7-90-142 (JINR, Dubna, 1990) p.99; Proc. R.A. Welch Foundation Conf. on chemical research XXXIV "Fifty years with transuranium elements", Houston 1990, p.279

[8] W. von Oertzen, Z. Phys. **A342** (1992) 177

[9] H. Bruchertseifer *et al.*, Abstracts of papers presented at the Int. IUPAC Symp. on the synthesis and properties of new elements, Dubna 1980, report D7-80-556 (JINR, Dubna, 1980) p.61

[10] V.I. Chepigin *et al.*, Abstracts of papers presented at the Int. IUPAC Symp. on the synthesis and properties of new elements, Dubna 1980, report D7-80-556 (JINR, Dubna, 1980) p.63

[11] Yu.Ts. Oganessian *et al.*, Nucl. Phys. **A239** (1975) 157

[12] Yu.Ts. Oganessian *et al.*, Nucl. Phys. **A273** (1976) 505

[13] G.N. Flerov *et al.*, Nucl. Phys. **A267** (1976) 359

[14] Yu.Ts. Oganessian *et al.*, Radiochim. Acta **37** (1984) 113

[15] T. Nomura, Proc. Int. Symp. on heavy-ion physics and its application, Lanzhou 1990, eds. W.O. Shen *et al.* (World Scientific, Singapore, 1991) p.349

[16] T. Shinozuka *et al.*, Int. Symp. "Towards a unified picture of nuclear dynamics", Nikko 1991, eds. Y. Abe *et al.*(AIP, New York, 1992) p.488

[17] H. Miyatake *et al.*, Nucl. Instr. Meth. Phys. Res. **B26** (1987) 309

[18] Yu.A. Lazarev *et al.*, Proc. Int. School-Seminar on heavy ion physics, Dubna 1993, report E7-93-274 (JINR, Dubna, 1993) vol.2, p.497

[19] A. Rytz, At. Data Nucl. Data Tables **47** (1991) 205

[20] C.M. Lederer and V.S. Shirley, eds., Table of isotopes, 7th Edition (Wiley-Interscience, New York, 1978)

[21] R. Hingmann *et al.*, Scientific Report 1984, GSI-85-1 (Darmstadt, 1985) p.88

[22] S.A. Kreek *et al.*, 1992 Annual Report, Nuclear Science Division, LBL-33333, UC-413 (Berkeley, 1993) p.61

[23] Yu.Ts. Oganessian, Proc. Int. School-Seminar on heavy ion physics, Alushta 1983, report D7-83-644 (JINR, Dubna, 1983) p.55

[24] Yu.A. Lazarev *et al.*, Europhys. Lett. **4** (1987) 893

[25] Yu.A. Lazarev *et al.*, Proc. Int. School-Seminar on heavy ion physics, Dubna 1989, report D7-90-142 (JINR, Dubna, 1990) p.208; Proc. 6th Int. Conf. on nuclei far from stability & 9th Int. Conf. on atomic masses and fundamental constants, Bernkastel-Kues 1992 (IOP, Bristol, 1993) p.739

[26] Yu.A. Lazarev *et al.*, Phys. Scripta **39** (1989) 422

[27] J.S. Fritz and G.R. Umbreit, Anal. Chim. Acta **19** (1958) 509

[28] A.N. Kuznetsov *et al.*, Prybory i Tekhnika Eksperimenta (in Russian) N^{0}1 (1987) 36; JINR preprint P13-85-637 (Dubna, 1985)

[29] V.B. Zlokazov, Nucl. Instr. Meth. **151** (1978) 303

[30] G. Münzenberg *et al.*, Z.Phys. **A302** (1981) 7

[31] Yu.Ts. Oganessian *et al.*, Nucl. Phys. **A239** (1975) 353

[32] H. Gäggeler *et al.*, Z.Phys. **A289** (1979) 415

[33] J.M. Nitschke *et al.*, Nucl. Phys. **A313** (1979) 236

[34] H. Gäggeler *et al.*, Z.Phys. **A316** (1984) 291

[35] Yu.P. Gangrsky *et al.*, Yadernaya Fizika (in Russian) **31** (1980) 306; transl.: Sov. J. Nucl. Phys. **31** (1980) 162

[36] D. Galeriu, J. of Phys. **G9** (1983) 309

[37] Yu.A. Lazarev *et al.*, in Heavy ion physics, scientific report 1991-1992, E7-93-57 (JINR, Dubna, 1993) p.57

[38] N.N. Kolesnikov and A.G. Demin, JINR preprint P6-9421 (Dubna, 1975); VINITI Dep. No.7309-B87, Tomsk (1987)

[39] R.Bass, Proc. Symp. on deep inelastic and fusion reactions with heavy ions, W. Berlin 1979, ed. W. von Oertzen, Lecture Notes in Physics **117** (1980) 281

[40] Yu.Ts. Oganessian *et al.*, Pis'ma Zh. Eksp. Theor. Fiz. (in Russian) **20** (1974) 580; transl.: JETP Lett. **20** (1974) 265

[41] P. Eskola *et al.*, Physica Fennica **8** (1973) 357

[42] O.A. Orlova *et al.*, Yadernaya Fizika (in Russian) **30** (1979) 618; transl.: Sov. J. Nucl. Phys. **30** (1979) 317

[43] Yu.Ts. Oganessian *et al.*, Proc Int. Symp. on physics and chemistry of fission, Jülich 1979 (IAEA, Vienna, 1980) vol. I, p.129

[44] F.P. Hessberger *et al.*, Scientific Report 1983, GSI-84-1 (Darmstadt, 1984) p.77

[45] F.P. Hessberger, thesis, report GSI-85-11 (Darmstadt, 1985)

[46] A. Ghiorso *et al.*, Nucl. Instr. Meth. Phys. Res. **A269** (1988) 192

[47] H.W. Gäggeler *et al.*, Nucl. Phys. **A502** (1989) 561c

[48] A. Türler *et al.*, Z.Phys. **A331** (1988) 363

[49] F.P. Hessberger *et al.*, Z.Phys. **A322** (1985) 557

[50] G. Münzenberg *et al.*, Z.Phys. **A315** (1984) 145

[51] K.-H. Schmidt and W. Morawek, Rep. Prog. Phys. **54** (1991) 949

[52] A. Ghiorso *et al.*, Phys. Rev. Lett. **22** (1969) 1317

[53] R.L. Hahn *et al.*, Phys. Rev. **C10** (1974) 1889

[54] N. Shinohara *et al.*, Phys. Rev. **C34** (1986) 909

[55] F.S. Stephens, J.R. Leigh and R.M. Diamond, Nucl. Phys. **A170** (1971) 321

[56] W.G. Winn, H.H. Gutbrod and M.Blann, Nucl. Phys. **A188** (1972) 423

[57] D. Vermeulen *et al.*, Z.Phys. **A318** (1984) 157